Gadolinium(III) Complexes of dota-Derived *N*-Sulfonylacetamides (H_4(dota-$NHSO_2R$) = 10-{2-[(R)sulfonylamino]-2-oxoethyl}-1,4,7,10-tetraazacyclododecane-1,4,7-triacetic Acid): A New Class of Relaxation Agents for Magnetic Resonance Imaging Applications

by **Silvio Aime***[a]), **Mauro Botta**[b]), **Giancarlo Cravotto**[c]), **Luca Frullano**[a])[1]), **Giovanni B. Giovenzana**[d]), **Simonetta Geninatti Crich**[a]), **Giovanni Palmisano**[e]), **and Massimo Sisti**[c])

[a]) Dipartimento di Chimica I.F.M., Università di Torino, Via P. Giuria 7, I-10125 Torino (fax: +39-011-6707855; e-mail: silvio.aime@unito.it)

[b]) Dipartimento di Scienze dell'Ambiente e della Vita, Università degli Studi del Piemonte Orientale 'A. Avogadro', Spalto Marengo 33, I-15100 Alessandria

[c]) Dipartimento di Scienza e Tecnologia del Farmaco, Università degli Studi di Torino, Via Giuria 9, I-10125 Torino

[d]) Dipartimento di Scienze Chimiche Alimentari, Farmaceutiche e Farmacologiche, Università degli Studi del Piemonte Orientale 'A. Avogadro',Via Bovio 6, I-28100 Novara

[e]) Dipartimento di Scienze Chimiche e Ambientali, Università degli Studi dell'Insubria, Via Valleggio 11, I-22100 Como

Dedicated to Professor *André E. Merbach* on the occasion of his 65th birthday

Four new ligands for lanthanide ions based on the H_3do3a (=1,4,7,10-tetraazacyclododecane-1,4,7-triacetic acid) structure and bearing one *N*-sulfonylacetamide arm were synthesized, *i.e.*, H_4dota-$NHSO_2R$ = 10-{2-[(R)sulfonylamino]-2-oxoethyl}-1,4,7,10-tetraazacyclododecane-1,4,7-triacetic acids **1a**–**e**. A ^{15}N-NMR study of the ^{15}N-labelled Eu^{3+} complex of one such ligands, **1d**, showed that the coordination of the *N*-sulfonylacetamide arm involves the carbonyl O-atom rather than the N-atom. The relaxometric properties of the corresponding Gd^{3+} complexes were investigated as a function of pH and temperature. These complexes have relaxivities in the range 4.5–5.3 mM^{-1} s^{-1}, at 20 MHz and 25°, and are characterized by a single H_2O molecule in their inner coordination sphere. The mean residence lifetime of this molecule is relatively long (500–700 ns) compared to other anionic complexes. The slow rate of H_2O exchange can be justified by the extensive delocalization of the negative charge on the *N*-sulfonylacetamide arm. The long residence time of the coordinated H_2O allowed the observation of the effect of the prototropic exchange on the relaxivity. The study of the interaction between the complex [Gd(**1e**)]- and HSA revealed a weak affinity constant highlighting the importance of a localized negative charge on the complex to promote a strong interaction with the protein.

Introduction. – Gadolinium complexes with polyaminopolycarboxylate ligands have been under intense scrutiny in the last decade because of their possible application as magnetic-resonance-imaging (MRI) contrast agents [1–3]. The large majority of the complexes considered for this purpose so far are based on octadentate ligands to ensure a high thermodynamic (and kinetic) stability. A Gd^{3+}-bound H_2O exchanging with tissue water determines, *via* the enhancement of the relaxation (T_1 and T_2) of the H_2O protons, the intensity of the water signal and thus the contrast in the images.

[1]) Present address: Chemistry Department, Northwestern University, 2145 Sheridan Road, Evanston, IL, 60208-3113, USA.

The theory describing the paramagnetic relaxation was developed by *Bloembergen*, *Solomon*, and *Morgan* [4–6] in the 1950s. With the support of this theory, it was early suggested that the efficiency of a MRI contrast agent is strongly dependent on a number of structural and dynamic parameters related to the coordination environment around the metal center and to the tumbling rate of the complex. As the value of these parameters for the commercial contrast agents is far from optimal, much research has been undertaken with the aim of attaining the high efficiencies predicted by the theory. The relaxation theory predicts that higher relaxation rates are obtained upon increasing the rotational correlation time of the Gd^{3+} complexes, which may be achieved by noncovalent or covalent binding of low-molecular-mass Gd^{3+} chelates to macromolecules or polymers [2]. In fact, many examples of lanthanide ligands functionalized with moieties apt to interact with serum proteins, particularly HSA (human serum albumin), are already known in the literature.

Here, we report the synthesis and physicochemical characterization of four new ligands bearing an *N*-sulfonylacetamide pendant arm (see **1a**–**e**) and their lanthanide complexes. The *N*-sulfonylacetamide moiety, possessing a negative charge at physiologic pH, represents an isosteric alternative to the carboxylic group. This offers the possibility to modulate several properties of the resulting complexes (charge, size, hydrophilicity, *etc.*) through a proper choice of the substituent at the S-atom by means of a synthetically convenient way. In this work, we considered three complexes bearing hydrophobic groups at the S-atom and investigated their binding affinity to HSA. HSA is known to tightly bind anionic lipids and, in general, it is well-established that most of the compounds interacting with HSA are hydrophobic organic anions [7][8]. It is thus interesting to investigate both the structure and the interaction with HSA of these new chelates.

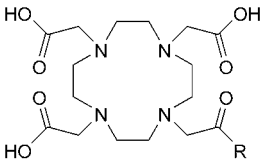

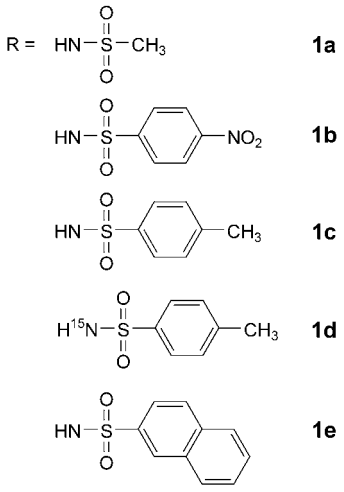

We studied the protonation pattern of one of the ligands and the coordination structure of its Eu^{3+} complex. The relaxometric parameters and the interaction with HSA of the gadolinium complexes were also assessed.

Results and Discussion. – Five *N*-sulfonylacetamide derivatives of H_4DOTA, **1a**–**e**, were prepared following the synthetic pathway outlined in the *Scheme*. First, the five 2-bromo-*N*-sulfonylacetamides **3a**–**e** were synthesized by reacting bromoacetyl bromide with the appropriate sulfonamide **2**. Then, these building blocks were used to alkylate do3a tri(*tert*-butyl) ester **4** (H_3do3a = 1,4,7,10-tetraazacyclododecane-1,4,7-triacetic acid) to give **5a**–**e**, and finally the desired ligands **1a**–**e** were obtained after deprotection with CF_3COOH.

To gain insight into the coordination mode of this type of ligands, the ^{15}N-labelled ligand **1d** was prepared starting from the commercially available *p*-toluenesulfon-(^{15}N)amide (= 4-methylbenzenesulfon(^{15}N)amide).

Scheme

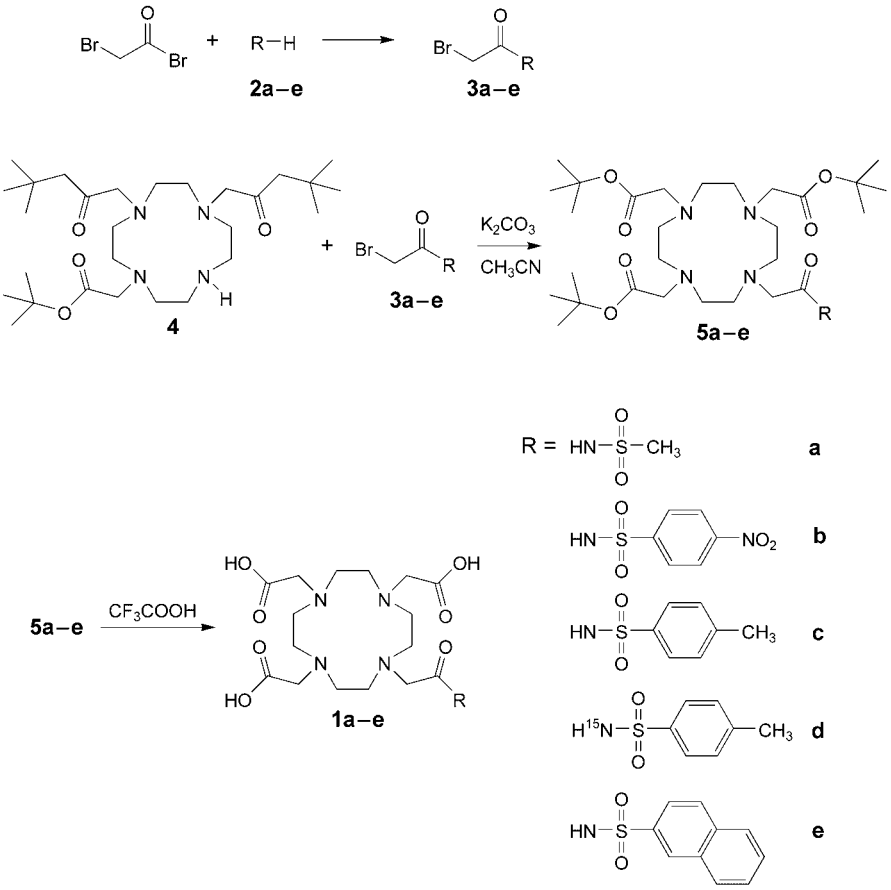

The Gd^{3+} complexes were synthesized by stepwise addition of $GdCl_3 \cdot 6\,H_2O$ to an aqueous solution of the ligand up to the stoichiometric ratio, while maintaining the pH of the solution at 6.0 with 1M NaOH. The formation of the complex was monitored by measuring the solvent proton relaxation rate ($1/T_1$) at 20 MHz and 25°.

Microscopic Protonation Sequence. The information obtainable from high-resolution NMR spectroscopy can be used to assess the value of the protonation constants and the sequence of protonation in polyaminocarboxylate ligands. The protonation constants K_n can be determined by fitting the variation with pH of the chemical shift for the various proton resonances, δ_i, to *Eqn. 1*, where χ_n is the molar fraction of the *n*-protonated species and δ_n are their intrinsic chemical shifts [9]. Combining *Eqn. 1* with *Eqn. 2* thus allows the determination of K_n.

$$\delta_{\mathrm{i}} = \sum_n \chi_n \delta_n \tag{1}$$

$$K_n = \frac{\chi_{n-1}[\mathrm{H}^+]}{\chi_n} \tag{2}$$

It is well known that the protonation state of a basic site influences the NMR shielding constant of adjacent nuclei. In particular, the protonation of a basic site induces a downfield shift of the ^{1}H-NMR resonances of adjacent protons. The magnitude of this shift depends upon the nature, the proximity, and the fraction of protonation of the basic site. *Sudmeier* and *Reilley* determined a series of shielding constants, or protonation shifts, for various model compounds and found for methylene groups in the moieties CH_2COO^-, CH_2NR_2, and $CH_2CH_2NR_2$ values of 0.2, 0.75, and 0.35 ppm, respectively [9][10].

The plot of the ^{1}H-NMR resonances of ligand **1b** (*Fig. 1*) as a function of pH are reported in *Fig. 2*. Although, from this NMR titration experiment it is not possible to precisely determine the number of protons involved in a given protonation step, by analogy with similar data on related ligands, we may assume that, in the pH range 8–10, two protonations occur with similar constants ($pK_1 \approx pK_2 = 8.77 \pm 0.01$). Likely, these two protons are used to protonate two amino groups in '*trans*' position to each other to minimize the electrostatic repulsion. This is consistent with the behavior reported for other cyclen derivatives [11]. The fact that the protons *1*, *4*, *5*, and *7* (see *Fig. 1*)

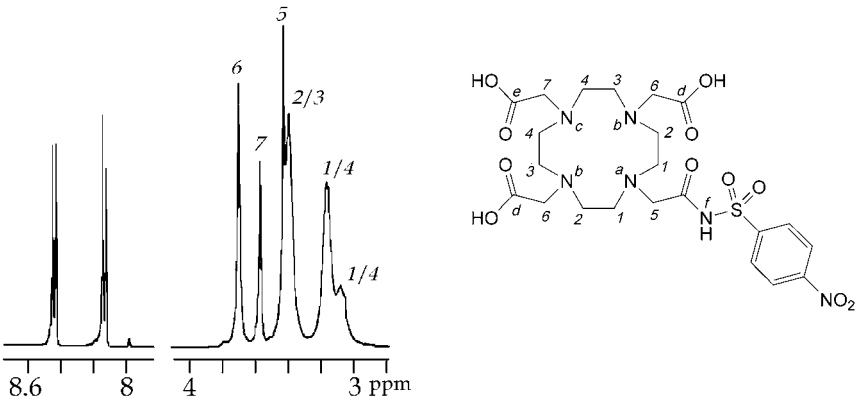

Fig. 1. *H-NMR Spectrum of ligand* **1b** *in D_2O, at 400 MHz, 25°, and pH 7.0.* Arbitrary numbering.

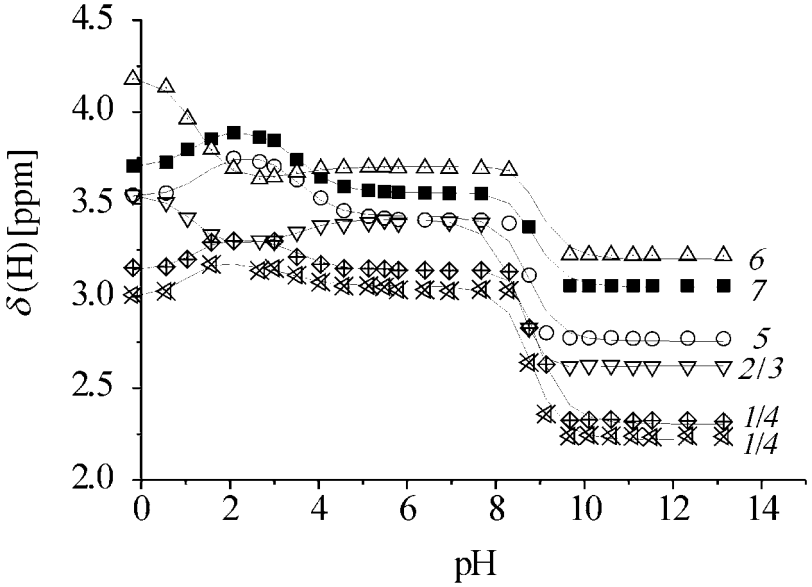

Fig. 2. *pH Dependence of the* ^{1}*H-NMR resonances of ligand* **1b** *recorded at 400 MHz and 25°*. The curves passing through the experimental values are the result of a best-fit procedure to *Eqns. 1* and *2*. Arbitrary numbering of protons according to *Fig. 1*.

experience the largest shift indicates that the highest proton density is present on the N-atoms *a* and *c*, although a significant amount of proton density is also located on the N-atom *b*. The first protonation constant for this ligand is markedly lower than that reported for H_4dota (=1,4,7,10-tetraazacyclododecane-1,4,7,10-tetraacetic acid) ($pK_1 = 11.08 \pm 0.07$) [11]. The next protonation event occurs at a pH close to 4 ($pK_3 = 3.58 \pm 0.06$). The trend in the chemical shift of the various resonances seems to indicate that this proton is localized on the carboxyl group *d*. The upfield shift of the protons *2*, *3*, and *6*, instead of the expected downfield shift, indicates that the protonation of the carboxylate group induces a shift of the proton density from the N-atom *b* to *a* and *c*, whose protonated forms can be stabilized by H-bonding interaction with the negatively charged acetate or *N*-sulfonylacetamide groups. The shift due to the deprotonation of the amino group dominates the effect originating from the protonation of the carboxylate group. This is confirmed by the simultaneous downfield shift of the resonances *1*, *4*, *5*, and *7* indicating an increased proton density on the N-atoms *a* and *c*.

After the second protonation of the carboxylate groups *d* ($pK_4 = 1.88 \pm 0.22$), the addition of the last two protons to the carboxylate *e* and to the *N*-sulfonylacetamide group ($pK_5 = 0.96 \pm 0.09$, $pK_6 = 0.45 \pm 0.40$) restores the initial proton distribution on the ring N-atoms. This is supported by the upfield shift of the resonances *1*, *4*, *5*, and *7* due to the decreased proton density on the N-atoms *a* and *c* and by the downfield shift of the resonances *2*, *3*, and *6* originating from the increased proton density on the N-atom *b*.

Coordination Mode. The magnitude of the lanthanide-induced shift (LIS) can be used to help identify of the donor atoms of the ligand in a complex. The LIS, the difference between the chemical-shift values of a nucleus in the paramagnetic complex and in a corresponding diamagnetic derivative, is given by the sum of a contact (Δ_c), a pseudocontact (Δ_p), and a diamagnetic (Δ_d) contribution (*Eqn. 3*) [12][13].

For the atoms directly bound to the paramagnetic Ln^{3+} ions, the contact contribution is generally very large and normally dominates the LIS. Therefore, for paramagnetic Ln^{3+} complexes with ligands containing multifunctional groups, the donor sites can be easily recognized by the magnitude of their LIS. However, a large LIS is invariantly accompanied by extensive line-broadening, which may prevent the detection of the resonance.

$$\Delta = \Delta_c + \Delta_p + \Delta_d \tag{3}$$

To investigate the coordination geometry of the *N*-sulfonylacetamide pendant arm, ligand **1d** was synthesized and studied by ^{15}N-NMR. The δ (^{15}N) of the ^{15}N-labelled **1d** and of the corresponding La^{3+} and Eu^{3+} complexes shows diamagnetic and paramagnetic contributions of $+11$ and -23 ppm, respectively (*Fig. 3*). From literature data on N-atoms directly coordinated to Eu^{3+}, a ^{15}N LIS of the order of -1500 ppm was expected [14]. Furthermore, the linewidth at half height of the ^{15}N resonance for [Eu(**1d**)]$^-$ results to be only 20.3 Hz. Both the small LIS and paramagnetically induced line broadening clearly indicate that the *N*-sulfonylacetamide group coordinates the Ln^{3+} cations through the carboxyl group. Thus, we may safely suggest a coordination geometry of the type represented in *Fig. 4*.

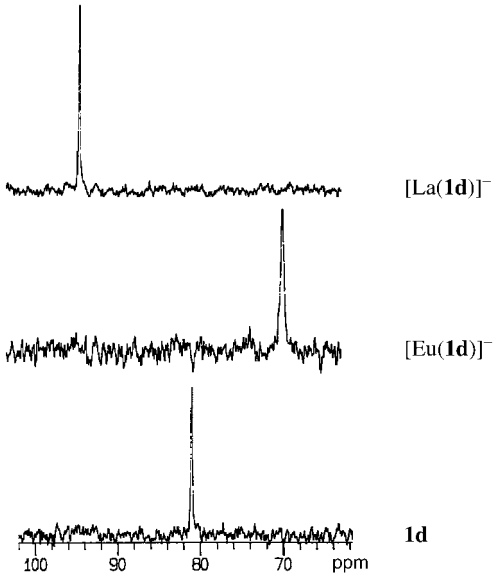

Fig. 3. *^{15}N-NMR Spectra of [La(**1d**)]$^-$, [Eu(**1d**)]$^-$, and **1d** at 40.53 MHz and 25°*

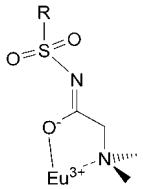

Fig. 4. *Schematic representation of the lanthanide coordination by the* N-*sulfonylacetamide arm*

Relaxometric Characterization of the Gd^{3+} Complexes. The ability of a paramagnetic complex to accelerate the NMR relaxation rates of the nuclei of the solvent water molecules is commonly expressed in terms of relaxivity, r_{ip} ($i=1,2$) [1–3]. This parameter represents the enhancement of the proton relaxation rate of an aqueous 1 mM solution of the paramagnetic complex with respect to pure water.

The relaxivities of the four complexes, as measured at 20 MHz and 25°, are 4.5, 5.0, 5.1, and 5.3 mM^{-1} s^{-1} for [Gd(**1a**)]$^-$, [Gd(**1b**)]$^-$, [Gd(**1c**)]$^-$, and [Gd(**1e**)]$^-$, respectively. These values are similar to those typical for complexes of similar size and with one inner-sphere H_2O molecule and suggest the presence of a single water molecule ($q=1$) coordinated to the metal center also for [Gd(**1a**–**e**)]$^-$. The complexes [Gd(**1a**)]$^-$, [Gd(**1b**)]$^-$, and [Gd(**1c**)]$^-$ showed a similar pH dependence of the relaxivity at 20 MHz and 25°. The fairly constant relaxivity in the pH range 2–12 implies that no changes in the structure and in the hydration number occur in this interval. On the other hand, at very low and very high pH values, there is a clear increase in relaxivity.

This enhancement of r_{ip} is too small to be ascribed to a change in the hydration number of the complex. Most likely, it arises from acid- and base-catalyzed activation of the prototropic exchange, leading to a more-efficient paramagnetic relaxation. However, for the change in relaxivity observed at pH < 2, a contribution due to partial decomplexation of the metal chelate cannot be completely ruled out.

The activation of the proton exchange on the coordinated H_2O molecule (prototropic exchange process) has the effect to shorten the effective residence lifetime, τ_M, of the water protons. This phenomenon has already been observed in Gd^{3+} complexes characterized by an exceedingly long residence lifetime of the H_2O molecule, where the activation of the prototropic exchange is able to remove the limiting effect on the relaxivity of a long τ_M value [15–18]. The occurrence of a τ_M value long enough so as to limit the relaxivity was confirmed by the temperature dependence of the relaxivity for the complexes [Gd(**1a**)]$^-$, and [Gd(**1b**)]$^-$ (*Fig. 5*).

The profile can be split in two regions; at high temperatures ($T>30°$), the exponential decrease in relaxivity reflects the exponential decrease of the reorientational correlation time, τ_R, with temperature. At lower temperatures ($T<30°$), the relaxivity profile flattens out as a result of the increase in τ_M that becomes comparable to or shorter than T_{1M} and thus quenches the relaxivity ($T_{1M} \leq \tau_M$; slow exchange regime). The comparison with the analogous profile of [Gd(dota)]$^-$ indicates that the *N*-sulfonylacetamide complexes are characterized by a slower rate of H_2O exchange.

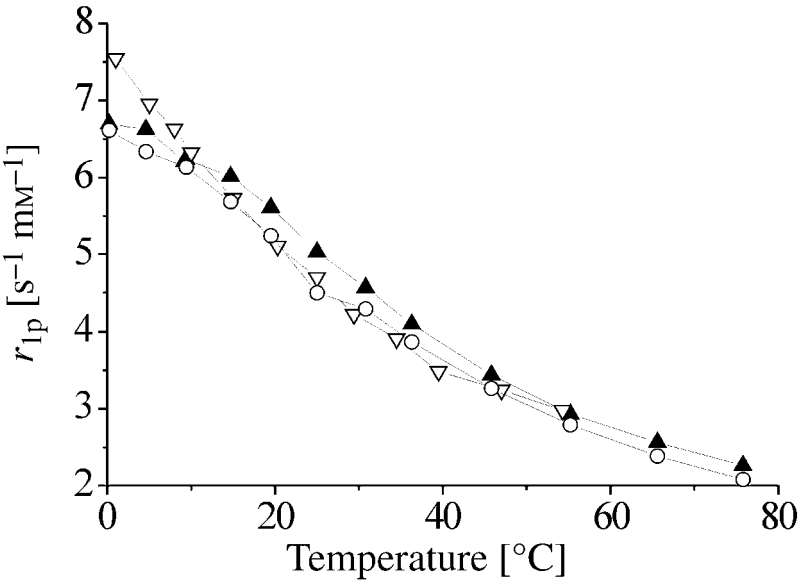

Fig. 5. *Temperature dependence of* r_{1p} *for [Gd(***1a***)]*$^-$ (○), *[Gd(***1b***)]*$^-$ (▲), *and [Gd(*dota*)]*$^-$ (▽).

To emphasize the effects associated with the activation of the prototropic exchange, the pH dependence of the relaxivity for the complexes [Gd(**1a**)]$^-$, and [Gd(**1b**)]$^-$ was also measured at low temperature (0.1°), where the H_2O-exchange rate is lower (*Fig. 6*). The exchange lifetime of H_2O protons is strongly pH-dependent, being very long at neutral pH (on the order of ms) and significantly shorter (of the order of ns) either in acidic or basic conditions. The prototropic exchange process may be adequately treated as a pseudo-first-order mechanism, characterized by a rate constant k_{ip}, the values of which for pure water at 301 K were reported to be in the range $4.1 - 7.1 \cdot 10^9\ s^{-1}\,M^{-1}$ and $2.2 - 4.3 \cdot 10^9\ s^{-1}\,M^{-1}$ for the acidic ($k_{ex,a}$) and basic ($k_{ex,b}$) catalysis, respectively [19]. When the exchange of the entire H_2O molecule is fast, the contribution arising from the prototropic exchange can be neglected. However, when the exchange of the H_2O molecule is slow, the prototropic exchange can contribute significantly to the observed relaxivity under basic or acidic conditions. The pH dependence of the relaxivity can, therefore, be fitted by using *Eqn. 4*, where r_1^{os} and r_1^{os} are the inner- and outer-sphere components of the relaxivity, C_t is the molar concentration of the metal complex, q the hydration number, and T_{1M} the longitudinal relaxation time of the protons of the bound H_2O molecule [1–3].

It is assumed that T_{1M} does not vary with pH. The pH dependence of the relaxivity of the complexes [Gd(**1a**)]$^-$ and [Gd(**1b**)]$^-$ was measured at 0.1° and 20 MHz, and the values of T_{1M}, τ_M, $k_{ex,a}$, and $k_{ex,b}$ obtained from the best fit of the data are reported in *Table 1* and compared with those obtained for the complex [Gd(dota)]$^-$ under identical experimental conditions. In the pH region around neutrality, the relaxivity is mainly dominated by the exchange rate of the whole H_2O molecule and thus is slightly higher

for [Gd(dota)]$^-$, this complex being characterized by a faster rate of exchange. At high (usually > 9) or low pH (usually < 3) values, the H_2O-exchange rate is no longer a factor limiting the relaxivity due to the activation of the prototropic exchange. Under these conditions, r_{1p} is primarily controlled by τ_R, and then the higher relaxivity observed for [Gd(**1a**)]$^-$ and [Gd(**1b**)]$^-$ can be explained in terms of the higher relative molecular mass of these two complexes.

$$r_{1p} = r_1^{os} + r_1^{is} = \frac{C_t \cdot q}{55.56 \cdot \left(T_{1M} + \frac{1}{k_{ex} + k_{exa} \cdot [H^+] + k_{exb} \cdot [OH^-]} \right)} + r_1^{os} \qquad (4)$$

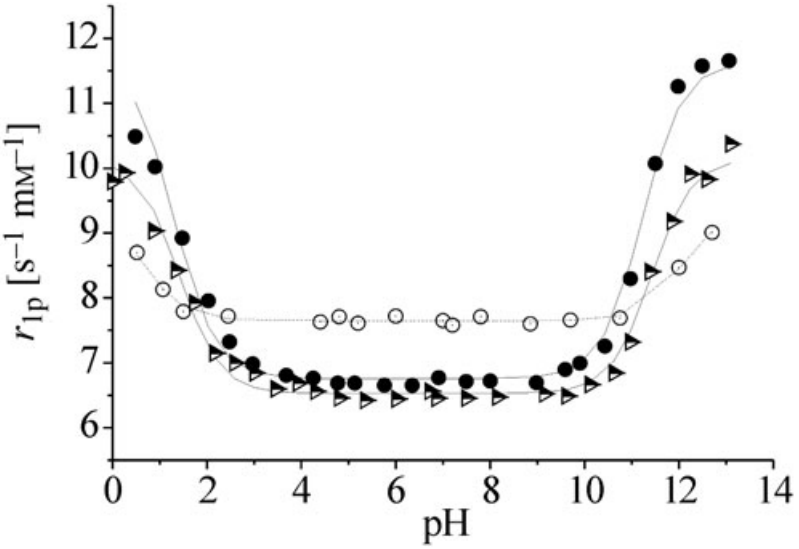

Fig. 6. *pH Dependence of the longitudinal water proton relaxivity* (r_{1p}) *for a 1 mM solution* (20 MHz, 0.1°) *of [Gd(***1a***)]*$^-$ (▷), *[Gd(***1b***)]*$^-$, (●), *and [Gd(*dota*)]*$^-$ (⊙). The lines through the data points are the result of a best fitting procedure to *Eqn. 4*.

Table 1. *Best-Fit Parameters Obtained from the Analysis of the pH Dependence of the Relaxivity for* [Gd(**1a**)]$^-$, [Gd(**1b**)]$^-$ *and* [Gd(dota)]$^-$ *at 0.1° and 20 MHz*

	[Gd(**1a**)]$^-$	[Gd(**1b**)]$^-$	[Gd(dota)]$^-$
T_{1M} [10^{-6} s]	2.83 ± 0.05	2.34 ± 0.05	3.4 ± 0.13
k_{ex} [10^5 s^{-1}]	2.65 ± 0.06	2.45 ± 0.07	6.02 ± 0.07
k_{exb} [10^8 s^{-1}]	2.38 ± 0.31	4.10 ± 0.61	0.79 ± 0.16
k_{exa} [10^7 s^{-1}]	1.63 ± 0.21	1.41 ± 0.21	0.43 ± 0.07
r_2^{os} [s^{-1}M^{-1}]	3.80 ± 0.05	3.96 ± 0.07	4.12 ± 0.09

Determination of the Water-Exchange Lifetime τ_M. An accurate estimate of the exchange lifetime of the H_2O molecules directly coordinated to the metal center, in a Gd^{3+} chelate, can be obtained from the temperature dependence of the transverse relaxation rate of the H_2O ^{17}O nuclei [1][20][21].

Fig. 7 shows the temperature dependence of the paramagnetic contribution to the transverse relaxation rate, R_2, for [Gd(**1b**)]$^-$, measured at pH 7 and at 2.12 T and normalized to 50 mM concentration. For comparison, the corresponding profile of the complex [Gd(dota)]$^-$ is also shown [22]. The curves exhibit a maximum that is characteristic of the changeover between the fast-exchange region, at high temperature, where R_2 is mainly dominated by electronic relaxation, and the slow-exchange region, at low temperature, where the transverse relaxation rate is dominated by τ_M. The relaxation rates measured for the two complexes are similar but the maximum for [Gd(**1b**)]$^-$ is shifted towards higher temperatures, to indicate a slower rate of H_2O exchange. A best-fit procedure of the experimental data obtained for the three complexes investigated ([Gd(**1a**)]$^-$, [Gd(**1b**)]$^-$, and [Gd(**1c**)]$^-$) according to the standard theory provides values for the exchange lifetimes on the order of a few hundred ns (*Table 2*) at 25° [19]. The calculated exchange rates are slower than that reported for the negatively charged [Gd(dota)]$^-$, but rather similar to those observed for several neutral Gd^{3+} complexes of monoamide derivatives of dota [2][23]. A possible explanation for this behavior can be the high delocalization of the negative charge on the *N*-sulfonylacetamide moiety, which results in a higher enthalpy of activation for the dissociation of the Gd–O_w bond with respect to the corresponding carboxylate derivative.

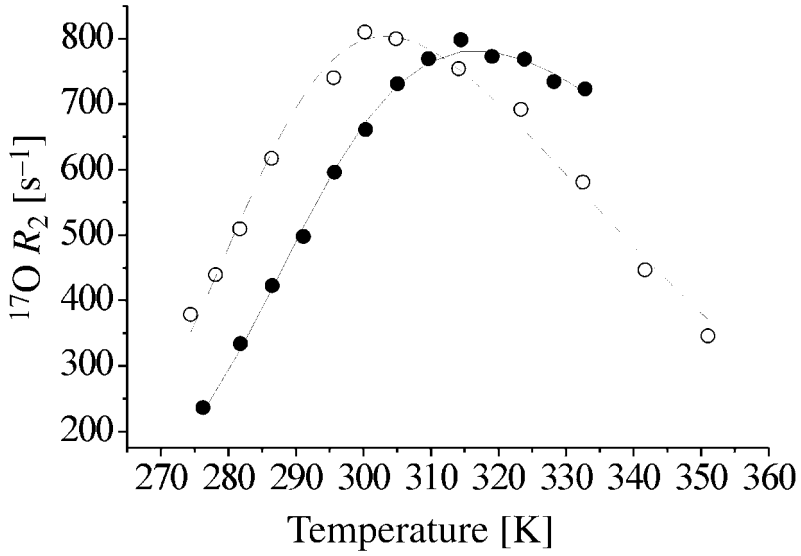

Fig. 7. *Temperature dependence of the transverse water ^{17}O relaxation rate at 9.4 T and pH 7 for 50 mM solutions of [Gd(**1b**)]$^-$* (●) *and [Gd(dota)]$^-$* (○). The solid curve through the data points was calculated with the parameters reported in *Table 2*.

For Gd-based MRI contrast agents, a long exchange lifetime represents a drawback since it often limits the attainable relaxivities. However, this disadvantage turns into an advantage for contrast agents based on the chemical exchange saturation transfer

Table 2. *Best-Fit Parameters Obtained from the Analysis of the Temperature Dependence of the ^{17}O-NMR Transverse Relaxation Rate, R_2, of the Gd^{3+} Complexes in Aqueous Solution at pH 7*

	q	Δ^2 [$s^{-2}/10^{19}$]	τ_v [ps]	τ_M^{25} [ns]	ΔH_m [kJ mol^{-1}]	ΔH_v [kJ mol^{-1}]
[Gd(**1a**)]$^-$	1	1.7 ± 0.5	9 ± 3	507 ± 20	52 ± 0.5	2.7 ± 2
[Gd(**1b**)]$^-$	1	2.1 ± 0.3	15 ± 2	746 ± 35	44 ± 0.7	9.0 ± 3
[Gd(**1c**)]$^-$	1	3.7 ± 0.4	14 ± 3	613 ± 40	59 ± 0.8	1.8 ± 1
[Gd(dota)]$^-$	1	1.4 ± 0.2	7 ± 2	244 ± 16	50 ± 0.3	1.0 ± 0.6

(CEST) mechanism. This new class of contrast agents is based on paramagnetic Ln^{3+} cations other than Gd^{3+} that are able to shift the resonance of the coordinated H_2O protons substantially away from the resonance of the bulk H_2O, without inducing an extreme line broadening [24][25]. All the complexes so far investigated are based on tetramide derivatives of dota. The H_2O-exchange lifetimes typical of the mono-*N*-sulfonylacetamide derivatives of dota investigated in this study are still too short to find a successful application in CEST MRI procedures. Nevertheless, the observed values suggest that the replacement of acetate with *N*-sulfonylacetamide arms could slow the H_2O exchange enough to make the appropriate complexes potentially useful for CEST applications.

Finally, the measurement of the exchange lifetime by ^{17}O-NMR at pHs 3.5 and 7.0 for [Gd(**1a**)]$^-$ afforded very similar values, thus confirming once more that the relaxivity change as a function of pH at 20 MHz arises exclusively from the activation of the prototropic exchange.

Binding to HSA. MRI Contrast agents that are currently used in clinical practice are Gd^{3+} complexes characterized by a relative molecular mass between 500 and 600. Complexes of this size are characterized by a relaxivity that is mainly controlled by the fast molecular mobility in solution. The most widely adopted strategy to reduce the molecular rotational tumbling, and thus increase the relaxivity, exploits the non-covalent binding of the small paramagnetic complexes to macromolecular substrates [26–28]. HSA has been widely employed to this purpose because it represents the most-abundant serum protein, and it can be used as a target by contrast agents designed for angiographic applications [2][27]. Strong interaction between HSA and the contrast agent is pursued not only for increasing the relaxivity but also for attaining longer residence lifetimes in the bloodstream.

The interaction between paramagnetic complexes and HSA can be conveniently investigated at a fixed frequency by means of the proton-relaxation-enhancement (PRE) method [26–28]. The enhancement of the NMR H_2O proton relaxation in the presence of the macromolecular substrate is used to obtain reliable values for the binding constant (K_A) and the relaxivity of the macromolecular adduct (r_{1b}). It is known that the presence of hydrophobic substituents on the surface of the complex and an overall negative charge play an important role in promoting a strong interaction with HSA. This prompted us to study the noncovalent binding of [Gd(**1e**)]$^-$ with HSA.

This interaction was studied by measuring, at the fixed frequency of 20 MHz and at 25°, the longitudinal H_2O proton relaxation rate of a $1.98 \cdot 10^{-4}$ M aqueous solution (50 mM HEPES) of the complex in the presence of increasing concentrations of the

protein (*Fig. 8*). The observed relaxation rate can be expressed in terms of *Eqn. 5*, where r_{1p}^{free} and r_{1p}^{bound} are the relaxivities of the free complex and of the complex–HSA adduct at 25°, respectively, and R_{1d} represents the diamagnetic contribution (charges are omitted for the sake of clarity). The interaction between the complex and the protein can be represented by the equilibrium of *Eqn. 6*, characterized by the formation constant K_A (*Eqn. 7*), where n represents the number of equivalent and independent interaction sites. By combining *Eqn. 5* with *Eqn. 7*, it is possible to evaluate the product $K_A \cdot n$ and r_{1p}^{bound}. The affinity constant of [Gd(**1e**)]$^-$ for HSA is rather weak ($K_A \cdot n = 4 \cdot 10^2$), whereas the relaxivity of the macromolecular adduct, [Gd(**1e**)]–HSA, is 24.4 mM^{-1} s^{-1}. The K_A value found for this complex is significantly smaller than those found for other anionic complexes. On the basis of the available information, it is not possible to ascribe the limited binding to structural constraints or to the charge delocalization in the *N*-sulfonylacetamide moiety.

$$R_1^{obs} = r_{1p}^{free}[\mathrm{Gd} - (\mathbf{1e})] + r_{1p}^{bound}[\mathrm{Gd} - (\mathbf{1e}) - \mathrm{HSA}] + R_{1d} \tag{5}$$

$$[\mathrm{Gd}(\mathbf{1e})] + \mathrm{HSA} \leftrightarrow [\mathrm{Gd}(\mathbf{1e})] - \mathrm{HSA} \tag{6}$$

$$K_A = \frac{[[\mathrm{Gd}(\mathbf{1e})] - \mathrm{HSA}]}{[[\mathrm{Gd}(\mathbf{1e})]] \cdot n \cdot [\mathrm{HSA}]} \tag{7}$$

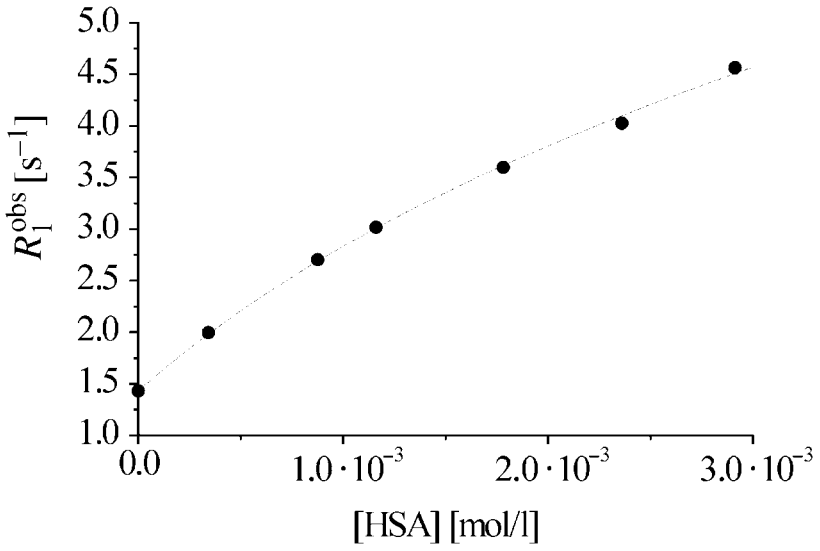

Fig. 8. *Plot of the water proton relaxation rate of a 0.1 mM [Gd(**1e**)]$^-$ solution as function of the HSA concentration* (20 MHz, 25°, in 50 mM phosphate buffer)

The relaxivity of the [Gd(**1e**)]–HSA supramolecular adduct is very close to the value that is predicted by the *Solomon–Bloembergen–Morgan* theory by using the parameters determined for the other Gd^{3+} complexes studied and by using a τ_r value of

30 ns. This represents the maximum attainable value in the presence of the relatively low H_2O-exchange rate shown by $[Gd(\mathbf{1e})]^-$.

Conclusions. – The *N*-sulfonylacetamide group represents an isosteric equivalent of the acetic acid group and thus acts as a good donor group for lanthanide(III) cations. A new series of Ln complexes (Ln = Eu, Gd) containing an *N*-sulfonylacetamide moiety at the do3a scaffold were prepared and characterized in terms of solution coordination mode and relaxometric behavior. The replacement of an acetic acid by an *N*-sulfonylacetamide moiety on the dota basic structure results in a substantial decrease of the rate of H_2O exchange. Even though these complexes have a net negative charge at neutral pH, the exchange lifetimes are similar to those of related neutral complexes. The high delocalization of the charge on the *N*-sulfonylacetamide moiety may be at the origin of this effect. The long values of the mean residence lifetimes of the coordinated H_2O molecule (τ_M) allowed the observation of the effects of the prototropic exchange at high and low pH.

The slow H_2O exchange, typical of these complexes, represents a serious drawback for the development of Gd-based MRI contrast agents but at the same time, it provides new insights for the design of novel CEST agents.

The authors thank Dr. *Joop Peters*, TU Delft, The Netherlands, for useful discussions. Financial support from *MUIR* (*FIRB* project) and from *Bracco Imaging SpA*, Milano, Italy, is gratefully acknowledged.

Experimental Part

General. HSA (crystallized and lyophilized) was purchased from *Sigma*, St. Louis, USA, and was used without any further purification. The molecular mass was assumed to be 69 kDa [17]. *p*-Toluenesulfon(^{15}N)amide (> 99% ^{15}N) was purchased from *Isotec Inc.*, Miamisburg, USA, and used as received. All other chemicals were of anal. grade and were purchased from *Sigma-Aldrich*, St. Louis, USA. M.p.: *Büchi 520* apparatus; uncorrected. NMR Spectra: *Bruker AC-200* (200 (^{1}H) and 50.2 MHz (^{13}C) resp.) and *Jeol EX-400* (400 MHz (^{1}H and ^{15}N)) spectrometers; δ in ppm, *J* in Hz; NMR pH titration in D_2O (99.8%), the pD being adjusted with DCl or CO_2-free NaOD (*Sigma*).

The longitudinal H_2O proton relaxation rates were measured on the *Stelar Spinmaster* spectrometer (*Stelar*, Mede (PV), Italy) operating at 20 MHz, by means of the standard inversion-recovery technique (16 experiments, 2 scans). A typical 90° pulse width was 3.5 μs, and the reproducibility of the T_1 data was 0.5%. The temp. was controlled with a *Stelar VTC-91* air-flow heater equipped with a copper-constantan thermocouple (uncertainty of 0.1°).

Variable-temp. ^{17}O-NMR measurements were recorded on a *Jeol EX-400* (9.4 T) spectrometer, equipped with a 5-mm probe, by using D_2O as external lock. Experimental settings were: spectral width 10880 Hz, pulse width 7 μs, acquisition time 10 ms, 256 scans, no sample spinning. Solns. containing 2.6% of ^{17}O isotope (*Yeda*, Israel) were used. The transverse relaxation rates (R_2^{obs}) were calculated from the signal width at half-height. The paramagnetic contribution, R_2, was obtained by subtracting from the data the signal width at half-height of a soln. of H_2O at pH 7 with identical ^{17}O enrichment ($R_2 = R_2^{obse} - R_{2w}$).

Mass Spectra: *VG 7070-EQ* spectrometer; CI (isobutene) for ligands **1a**–**e**, FAB (*m*-nitrobenzyl alcohol or glycerol) for the other compounds; in *m*/*z*. Elemental analyses were performed with a *Perkin-Elmer 240* apparatus.

Naphthalene-2-sulfonamide (**2e**). Naphthalene-2-sulfonyl chloride (2.49 g, 11.0 mmol) and $(NH_4)_2CO_3$ were mixed and finely ground. The mixture was heated for 15 min at 100°, resulting in extensive foaming. The cooled residue was washed thoroughly with H_2O to remove ammonium salts. The crude product was purified by recrystallization from H_2O: 2.28 g (88%) of **2e**. M.p. 217–219°. ^{1}H-NMR ($CDCl_3$, 200 MHz): 8.20 (*s*, 1 H), 8.02 (br. *s*, 1 H); 7.91 (*s*, 1 H); 7.47–7.37 (*m*, 4 H); 7.14–7.02 (*m*, 2 H). ^{13}C-NMR ($CDCl_3$, 50.2 MHz): 140.6; 133.7; 131.5; 128.5; 127.8; 127.7; 127.3; 126.9; 125.7; 121.8.

2-Bromo-N-*sulfonylacetamides* **3a**–**e**: *General Procedure.* The sulfonamide **2a**–**d** (2 mmol) was suspended in anh. toluene (5 ml) (chlorobenzene for **2e**), bromoacetyl bromide (3–4 mmol) was carefully added dropwise, and the mixture was refluxed for 4–5 h. The product crystallized from the mixture upon cooling. It was separated by filtration and recrystallized from toluene in the case of **3a**–**c**. For the isolation of **3d**, **e**, the mixture was evaporated; the residue redissolved in sat. $NaHCO_3$ soln., the soln. filtered, and then the desired product precipitated by slow addition of conc. HCl soln.; further purification was achieved by recrystallization from toluene.

2-Bromo-N-*(methylsulfonyl)acetamide* (**3a**): Yield 47.5%. Colorless crystals. M.p. 102–104°. ^{1}H-NMR ($CDCl_3$, 200 MHz): 9.05 (*s*, 1 H); 3.96 (*s*, 3 H); 3.36 (*s*, 2 H). EI-MS: 217, 215 ($M^{+\bullet}$). Anal. calc. for $C_3H_6BrNO_3S$ (216.05): C 16.68, H 2.80, N 6.48; found C 16.50, H 3.01, N 6.45.

2-Bromo-N-*[(4-nitrophenyl)sulfonyl]acetamide* (**3b**). Yield 33.5%. Colorless crystals. M.p. 163–165°. ^{1}H-NMR ($CDCl_3$, 200 MHz): 9.01 (*s*, 1 H); 8.22 (*d*, $J = 8.8$, 2 H); 8.09 (*d*, $J = 8.8$, 2 H); 3.65 (*s*, 2 H). ^{13}C-NMR ($CDCl_3$, 50.2 MHz): 165.2 (*s*); 150.4 (*s*); 144.0 (*s*); 129.5 (*d*); 123.8 (*d*); 27.7 (*t*). EI-MS: 324, 322 ($M^{+\bullet}$). Anal. calc. for $C_8H_7BrN_2O_5S$ (323.12): C 29.74, H 2.18, N 8.67; found C 29.52, H 2.21, N 8.80.

2-Bromo-N-*[(4-methylphenyl)sulfonyl]acetylamide* (**3c**): Yield 91.5%. Colorless crystals. M.p. 114–116°. ^{1}H-NMR ($CDCl_3$, 200 MHz): 9.36 (*s*, 1 H); 7.98 (*d*, $J = 8.2$, 2 H); 7.36 (*d*, $J = 8.2$, 2 H); 3.85 (*s*, 2 H); 2.45 (*s*, 3 H). ^{13}C-NMR ($CDCl_3$, 50.2 MHz): 164.2 (*s*); 145.6 (*s*); 134.5 (*s*); 129.7 (*d*); 128.5 (*d*); 27.8 (*t*); 21.6 (*t*). EI-MS: 293, 291 ($M^{+\bullet}$). Anal. calc. for $C_9H_{10}BrNO_3S$ (292.15): C 37.00, H 3.45, N 4.79; found C 36.91, H 3.61, N 4.67.

2-Bromo-N-*[4-methylphenyl)sulfonyl]acetyl(^{15}N)amide* (**3d**). Yield 70.5%. Colorless crystals. M.p. 115–116°. ^{1}H-NMR ($CDCl_3$, 200 MHz): 9.38 (*s*, 1 H); 7.98 (*d*, $J = 8.1$, 2 H); 7.38 (*d*, $J = 8.1$, 2 H); 3.84 (*s*, 2 H); 2.47 (*s*, 3 H). ^{13}C-NMR ($CDCl_3$, 50.2 MHz): 163.6 (*s*); 145.6 (*s*); 134.6 (*s*); 129.6 (*d*); 128.5 (*d*); 27.8 (*t*); 21.6 (*t*). EI-MS: 294, 292 ($M^{+\bullet}$). Anal. calc. for $C_3H_6Br^{15}NO_3S$ (293.14): C 36.88, H 3.44, N 5.12; found C 36.75, H 3.61, N 5.15.

2-Bromo-N-*(naphthalen-2-ylsulfonyl)acetamide* (**3e**): Yield 87.7%. White crystals. M.p. 132–134°. ^{1}H-NMR ($CDCl_3$, 200 MHz): 9.63 (br. *s*, 1 H); 8.72 (*s*, 1 H); 8.06–7.91 (*m*, 4 H); 7.73–7.63 (*m*, 2 H); 3.84 (*s*, 2 H). ^{13}C-NMR ($CDCl_3$, 50.2 MHz): 187.9 (*s*); 135.3 (*s*); 134.9 (*s*); 131.4 (*s*); 129.2 (*d*); 129.1 (*d*); 128.9–127.3 (4 *d*); 28.0 (*t*). EI-MS: 329, 327 ($M^{+\bullet}$). Anal. calc. for $C_{12}H_{10}BrNO_3S$ (328.18): C 43.92, H 3.07, N 4.27; found C 44.03, H 3.21, N 4.09.

Synthesis of **5a**–**e**: *General Procedure.* To a soln. of **4** (1 mmol) in DMF, finely powdered K_2CO_3 (3 mmol) followed by **3a**–**e** (1.5 mmol) were added, and the heterogeneous mixture was heated at 70–100° for 4–15 h (TLC (SiO_2, CH_2Cl_2/MeOH/conc. NH_3 soln. 9:1:0.1) monitoring). The mixture was diluted with CH_2Cl_2 (10 ml), filtered, and evaporated. Chromatography (silica gel) of the solid residue afforded pure **5a**–**e**.

*10-{2-[(Methylsulfonyl)amino]-2-oxoethyl}-1,4,7,10-tetraazacyclododecane-1,4,7-triacetic Acid Tri(*tert-*butyl) Ester* (**5a**): Yield 69.0%. White amorphous solid. M.p. 76–78°. ^{1}H-NMR ($CDCl_3$, 200 MHz): 3.01 (*s*, 3 H); 3.40–1.90 (*m*, 24 H); 1.41 (*s*, 27 H). ^{13}C-NMR ($CDCl_3$, 50.2 MHz): 177.2 (*s*); 172.1 (*s*); 172.0 (*s*); 81.6 (*s*); 81.5 (*s*); 59.2 (*t*); 55.8 (*t*); 55.5 (*t*); 50.5 (br. *s* (4 *t*)); 39.3 (*q*); 27.8 (*q*); 27.6 (*q*). CI-MS: 650 ($[M+H]^+$). Anal. calc. for $C_{29}H_{55}N_5O_9S$ (649.84): C 53.60, H 8.53, N 10.78; found C 53.52, H 8.70, N 10.80.

*10-{2-{[(4-Nitrophenyl)sulfonyl]amino}-2-oxoethyl}-1,4,7,10-tetraazacyclododecane-1,4,7-triacetic Acid Tri(*tert-*butyl) Ester* (**5b**): Yield 85.2%. Pale yellow amorphous solid. M.p. 63–65°. ^{1}H-NMR ($CDCl_3$, 200 MHz): 8.27 (*d*, $J = 8.8$, 2 H); 8.04 (*d*, $J = 8.8$ Hz, 2 H); 3.20–2.20 (*m*, 24 H); 1.45 (*s*, 18 H); 1.43 (*s*, 9 H). ^{13}C-NMR ($CDCl_3$, 50.2 MHz): 176.8 (*s*); 172.0 (*s*); 169.6 (*s*); 151.6 (*s*); 148.1 (*s*); 128.8 (*d*); 122.6 (*d*); 81.9 (*s*); 81.5 (*s*); 59.3 (*t*); 57.0 (*t*); 55.2 (*t*); 50.1 (br. *s* (4 *t*)); 28.0 (*q*); 27.7 (*q*). CI-MS: 757 ($[M+H]^+$). Anal. calc. for $C_{34}H_{56}N_6O_{11}S$ (756.91): C 53.95, H 7.46, N 11.10; found C 53.84, H 7.37, N 11.19.

*10-{2-{(4-Methylphenyl)sulfonyl]amino}-2-oxoethyl}-1,4,7,10-tetraazacyclododecane-1,4,7-triacetic Acid Tri(*tert-*butyl) Ester* (**5c**): Yield 53.2%. White amorphous solid. M.p. 75–77°. ^{1}H-NMR ($CDCl_3$, 200 MHz): 7.97 (*d*, $J = 8.0$, 2 H); 7.02 (*d*, $J = 8.0$, 2 H); 3.05–2.87 (*m*, 8 H); 2.16–2.05 (*m*, 16 H); 1.45 (*s*, 18 H); 1.41 (*s*, 9 H). ^{13}C-NMR ($CDCl_3$, 50.2 MHz): 176.1 (*s*); 172.0 (*s*); 171.8 (*s*); 142.7 (*s*); 138.9 (*s*); 129.1 (*d*); 126.3 (*d*); 81.6 (*s*); 81.4 (*s*); 59.7 (*t*); 56.1 (*t*); 55.3 (*t*); 50.2 (br. *s* (4 *t*)); 27.8 (*q*); 27.7 (*q*); 22.0 (*q*). CI-MS: 726 ($[M+H]^+$). Anal. calc. for $C_{35}H_{59}N_5O_9S$ (725.94): C 57.91, H 8.19, N 9.65; found C 57.78; H 8.26; N 9.70.

*10-{2-{[(4-Methylphenyl)sulfonyl](^{15}N)amino}-2-oxoethyl}-1,4,7,10-tetraazacyclododecane-1,4,7-triacetic Acid Tri(*tert-*butyl) Ester* (**5d**): Yield 64.6%. White amorphous solid. M.p. 73–77°. ^{1}H-NMR ($CDCl_3$, 200 MHz): 7.98 (*d*, $J = 8.0$); 7.04 (*d*, $J = 8.0$, 2 H); 3.20–2.10 (*m*, 24 H); 1.48 (*s*, 18 H); 1.42 (*s*, 9 H). ^{13}C-NMR ($CDCl_3$, 50.2 MHz): 176.2 (*s*); 171.9 (*s*); 171.8 (*s*); 142.5 (*s*); 138.8 (*s*); 129.1 (*d*); 126.5 (*d*); 81.5 (*s*); 81.4 (*s*); 59.4 (*t*); 56.2 (*t*); 55.5 (*t*); 50.3 (br. *s* (4 *t*)); 27.8 (*q*); 27.7 (*q*); 22.0 (*q*). CI-MS: 727 ($[M+H]^+$). Anal. calc. for $C_{35}H_{59}{}^{15}NN_4O_9S$ (726.93): C 57.83, H 8.18, N 9.77; found C 57.67, H 8.32, N 9.69.

*10-{2-[(Naphthalen-2-ylsulfonyl)amino]-2-oxoethyl}-1,4,7,10-tetraazacyclododecane-1,4,7-triacetic Acid Tr(*tert-*butyl) Ester* (**5e**): Yield 59.8%. White amorphous solid. M.p. 90–93°. ^{1}H-NMR ($CDCl_3$, 200 MHz): 8.60 (*d*,

$J = 1.4$, 1 H); 8.26 (*dd*, $J_1 = 8.6$, $J_2 = 1.7$, 1 H); 7.85–7.70 (*m*, 2 H); 7.64 (*d*, $J = 8.6$, 1 H); 7.48–7.34 (*m*, 2 H); 3.20–2.10 (*m*, 24 H); 1.46 (*s*, 18 H); 1.45 (*s*, 9 H). ^{13}C-NMR ($CDCl_3$, 50.2 MHz): 176.2 (*s*); 172.0 (*s*); 171.8 (*s*); 143.0 (*s*); 134.0 (*s*); 132.4 (*s*); 129.0 (2 *d*); 127.3–126.3 (4 *d*); 125.5 (*d*); 81.7 (*s*); 81.5 (*s*); 59.7 (*t*); 56.0 (*t*); 55.3 (*t*); 50.0 (br. *s* (4 *t*)); 27.8 (*q*); 27.7 (*q*). CI-MS: 762 ($[M+H]^+$). Anal. calc. for $C_{38}H_{59}N_5O_9S$ (761.98): C 59.90, H 7.80, N 9.19; found C 59.92, H 8.00, N 9.12.

Hydrolysis of **5a**–**e** *to* **1a**–**e**: *General Procedure.* A soln. of **5e**–**e** (1 mmol) in CF_3COOH (5 ml) was stirred for 24 h at r.t. The mixture was then evaporated, the residue redissolved in MeOH (3 ml), and the product precipitated by addition of an excess of Et_2O. The solid was washed twice with Et_2O and finally dried *in vacuo:* **1a**–**e**.

10-{2-[(Methylsulfonyl)amino]-2-oxoethyl}-1,4,7,10-tetraazacyclododecane-1,4,7-triacetic Acid (**1a**): White amorphous solid. M.p. 200–201° (dec.). ^{1}H-NMR (D_2O, 200 MHz): 3.72 (*s*, 4 H); 3.56 (*s*, 4 H); 3.45 (*s*, 4 H); 3.25–2.92 (*m*, 16 H); 3.11 (*s*, 3 H). ^{13}C-NMR (D_2O, 50.2 MHz): 176.1 (*s*); 173.9 (*s*); 172.2 (*s*); 58.0 (*t*); 56.3 (*t*); 55.4 (*t*); 53.5 (br. *s* (2 *t*)); 50.6 (br. *s* (2 *t*)); 43.0 (*q*). FAB-MS (pos.): 504 ($[M+Na]^+$), 482 ($[M+H]^+$). Anal. calc. for $C_{17}H_{31}N_5O_9S$ (481.53): C 42.40, H 6.49, N 14.54; found C 42.15, H 6.57, N 14.43.

10-{2-{[(4-Nitrophenyl)sulfonyl]amino}-2-oxoethyl}-1,4,7,10-tetraazacyclododecane-1,4,7-triacetic Acid (**1b**): White amorphous solid. M.p. 95–100° (dec.). ^{1}H-NMR (D_2O, 200 MHz): 8.28 (*d*, $J = 8.1$, 2 H); 8.04 (*d*, $J = 8.1$, 2 H); 3.80–3.40 (*m*, 8 H); 3.30–2.70 (*m*, 16 H). FAB-MS (pos.): 611 ($[M+Na]^+$), 589 ($[M+H]^+$). Anal. calc. for $C_{22}H_{32}N_6O_{11}S$ (588.59): C 44.89, H 5.48, N 14.28; found C 44.62, H 5.49, N 14.09.

10-{2-{[(4-Methylphenyl)sulfonyl]amino}-2-oxoethyl}-1,4,7,10-tetraazacyclododecane-1,4,7-triacetic Acid (**1c**): White amorphous solid. M.p. 175–179° (dec.). ^{1}H-NMR (D_2O, 200 MHz): 7.66 (*d*, $J = 8.2$, 2 H); 7.25 (*d*, $J = 8.2$, 2 H); 3.56–3.34 (*m*, 8 H); 3.16–2.80 (*m*, 16 H); 2.23 (*s*, 3 H). ^{13}C-NMR (D_2O, 50.2 MHz): 175.8 (*s*); 172.8 (*s*); 172.7 (*s*); 148.5 (*s*); 137.2 (*s*); 132.3 (*d*); 130.0 (*d*); 59.7 (*t*); 56.7 (*t*); 55.8 (*t*); 53.1 (br. *s* (2 *t*)); 50.7 (br. *s* (2 *t*)), 23.2 (*q*). FAB-MS (pos.): 580 ($[M+Na]^+$), 558 ($[M+H]^+$). Anal. calc. for $C_{23}H_{35}N_5O_9S$ (557.62): C 49.54, H 6.33, N 12.56; found C 49.45, H 6.48, N 12.53.

10-{2-{[(4-Methylphenyl)sulfonyl](^{15}*N)amino}-2-oxoethyl}-1,4,7,10-tetraazacyclododecane-1,4,7-triacetic Acid* (**1d**): White amorphous solid. M.p. 177–181° (dec.). ^{1}H-NMR (D_2O, 200 MHz): 7.70 (*d*, $J = 8.1$, 2 H); 7.30 (*d*, $J = 8.1$, 2 H); 3.60–3.46 (*m*, 8 H); 3.19–2.84 (*m*, 16 H); 2.27 (*s*, 3 H). ^{13}C-NMR (D_2O, 50.2 MHz): 175.7 (*s*); 172.7 (*s*); 172.6 (*s*); 148.6 (*s*); 137.2 (*s*); 132.3 (*d*); 130.0 (*d*); 57.9 (*t*); 56.7 (*t*); 55.7 (*t*); 53.0 (br. *s* (2 *t*)); 50.8 (br. *s* (2 *t*)); 23.2 (*q*). FAB-MS (pos.): 581 ($[M+Na]^+$), 559 ($[M+H]^+$). Anal. calc. for $C_{23}H_{35}{}^{15}NN_4O_9S$ (558.61): C 49.45, H 6.32, N 12.71; found C 49.44, H 6.51, N 12.63.

10-{2-[(Naphthalen-2-ylsulfonyl)amino]-2-oxoethyl}-1,4,7,10-tetraazacyclododecane-1,4,7-triacetic Acid (**1e**): White amorphous solid. M.p. 203–206° (dec.). ^{1}H-NMR (D_2O, 200 MHz): 8.26 (*m*, 2 H); 7.73–7.63 (*m*, 3 H); 7.39 (*m*, 2 H); 3.01–2.81 (*m*, 8 H); 3.53–2.68 (*m*, 16 H). FAB-MS (pos.): 616 ($[M+Na]^+$), 594 ($[M+H]^+$). Anal. calc. for $C_{26}H_{35}N_5O_9S$ (593.66): C 52.60, H 5.94, N 11.80; found C 52.47, H 6.07, N 11.73.

REFERENCES

[1] A. E. Merbach, E. Tóth, 'The Chemistry of Contrast Agents in Medical Magnetic Resonance Imaging', John Wiley & Sons, Chicester, 2001.
[2] P. Caravan, J. J. Ellison, T. J. McMurry, R. B. Lauffer, *Chem. Rev.* **1999**, *99*, 2293.
[3] S. Aime, M. Fasano, E. Terreno, *Chem. Soc. Rev.* **1998**, *27*, 19.
[4] I. Solomon, *Phys. Rev.* **1955**, *99*, 559.
[5] N. Bloembergen, *J. Chem. Phys.* **1957**, *27*, 572.
[6] N. Bloembergen, L. O. Morgan, *J. Chem. Phys.* **1961**, *34*, 842.
[7] T. Peters Jr., 'All About Albumin: Biochemistry, Genetics and Medical Applications', Academic Press, San Diego (USA), 1996.
[8] M. F. T. Koehler, K. Zobel, M. H. Beresini, L. D. Caris, D. Combs, B. D. Paasch, R. A. Lazarus, *Bioorg. Med. Chem. Lett.* **2002**, *12*, 2883.
[9] J. L. Sudmeier, C. X. Reilley, *Anal. Chem.* **1964**, *36*, 1698.
[10] C. F. Geraldes, A. M. Urbano, M. C. Alpoim, A. D. Sherry, K. T. Kuan, R. Rajagopalan, F. Maton, R. N. Muller, *Magn. Reson. Imaging* **1995**, *13*, 401.
[11] J. F. Desreux, E. Merciny, M. F. Loncin, *Inorg. Chem.* **1981**, *20*, 987.
[12] J. A. Peters, J. Huskens, D. J. Raber, *Prog. Nucl. Magn. Reson. Spectrosc.* **1996**, *28*, 283.
[13] C. F. G. C. Geraldes, C. Luchinat, in 'Metal Ions in Biological Systems', Eds. A. Sigel and H. Sigel, Marcel Dekker, Inc., Basel, 2003, Vol. 40, p. 513.

[14] R. M. Golding, M. P. Halton, *Aust. J. Chem.* **1972**, *25*, 2577.
[15] S. Aime, A. Barge, M. Botta, D. Parker, A. S. de Sousa, *J. Am. Chem. Soc.* **1997**, *119*, 4767.
[16] S. Aime, A. Barge, J. I. Bruce, M. Botta, J. A. K. Howard, J. M. Moloney, D. Parker, A. S. de Sousa, M. Woods, *J. Am. Chem. Soc.* **1999**, *121*, 5762.
[17] S. Aime, M. Botta, M. Fasano, E. Terreno, *Acc. Chem. Res.* **1999**, *32*, 941.
[18] S. Aime, E. Gianolio, A. Barge, D. Kostakis, I. C. Plakatouras, N. Hadjiliadis, *Eur. J. Inorg. Chem.* **2003**, 2045.
[19] B. Halle, G. Karlstroem, *J. Chem. Soc., Faraday Trans. 2* **1983**, *79*, 1031.
[20] D. H. Powell, O. M. Ni Dhubhghaill, D. Pubanz, L. Helm, Y. S. Lebedev, W. Schlaepfer, A. E. Merbach, *J. Am. Chem. Soc.* **1996**, *118*, 9333.
[21] U. Frey, A. E. Merbach, D. H. Powell, in 'Dynamics of Solutions and Fluid Mixtures by NMR', Ed. J.-J. Delpuech, John Wiley & Sons, Chichester, 1995, 263.
[22] K. Micksei, L. Helm, E. Brücher, A. E. Merbach, *Inorg. Chem.* **1993**, *32*, 3844.
[23] G. M. Nicolle, E. Toth, H. Schmitt-Willich, B. Raduchel, A. E. Merbach, *Chem.–Eur. J.* **2002**, *8*, 1040.
[24] S. Zhang, M. Merritt, D. E. Woessner, R. E. Lenkinski, A. D. Sherry, *Acc. Chem. Res.* **2003**, *36*, 783.
[25] S. Aime, D. Delli Castelli, E. Terreno, *Angew. Chem., Int. Ed.* **2002**, *41*, 4334.
[26] S. Aime, M. Botta, M. Fasano, E. Terreno, in 'The Chemistry of Contrast Agents in Medical Magnetic Resonance Imaging', Eds. A. E. Merbach and E. Tóth, John Wiley & Sons, Chicester, 2001, p. 193.
[27] S. Aime, A. Barge, M. Botta, E. Terreno, in 'Metal Ions in Biological Systems', Eds. A. Sigel and H. Sigel, Marcel Dekker, Inc., Basel, 2003, Vol. 40, p. 643.
[28] R. A. Dwek, 'Monographs on Physical Biochemistry: Nuclear Magnetic Resonance (N.M.R) in the Biochemistry. Applications to Enzyme Systems', Oxford University Press, New York, 1973, Vol. 3.

Received November 16, 2004